Design and test of a broadband split-and-delay unit for attosecond XUV-XUV pump-probe experiments.

Campi, Filippo; Coudert-Alteirac, Helene; Miranda, Miguel; Rading, Linnea; Manschwetus, Bastian; Rudawski, Piotr; L'Huillier, Anne; Johnsson, Per

Published in:
Review of Scientific Instruments

DOI:
10.1063/1.4941722

2016

Document Version:
Publisher's PDF, also known as Version of record

Design and test of a broadband split-and-delay unit for attosecond XUV-XUV pump-probe experiments

F. Campi,[a] H. Coudert-Alteirac,[a] M. Miranda, L. Rading, B. Manschwetus, P. Rudawski, A. L'Huillier, and P. Johnsson[b]
Department of Physics, Lund University, P.O. Box 118, 22100 Lund, Sweden

(Received 6 August 2015; accepted 27 January 2016; published online 16 February 2016)

We present the design of a split-and-delay unit for the production of two delayed replicas of an incident extreme ultraviolet (XUV) pulse. The device features a single grazing incidence reflection in combination with attenuation of remaining infrared light co-propagating with the XUV beam, offering a high throughput without the need of introducing additional optics that would further decrease the XUV flux. To achieve the required spatial and temporal stabilities, the device is controlled by two PID-controllers monitoring the delay and the beam pointing using an optical reference laser beam, making collimation of the beam by additional optics unnecessary. Finally, we demonstrate the stability of the split-and-delay unit by performing all-reflective autocorrelation measurements on broadband few-cycle laser pulses. [http://dx.doi.org/10.1063/1.4941722]

I. INTRODUCTION

The ultrafast dynamics of ionized and excited molecular systems depend on fundamental processes such as charge transfer or charge migration,[1–3] leading to chemical reactions and dissociation through, for instance, intramolecular rearrangements.[4] To achieve a deeper knowledge of the interplay between charge and structural dynamics in molecules, it is necessary to simultaneously probe the dynamics in the molecule on femtosecond and attosecond time scales, as these are the ones on which nuclear motion and charge dynamics occur, respectively.

One route to access the attosecond time scales involved in the above-mentioned processes is to use High-order Harmonic Generation (HHG), in which an intense infrared (IR) femtosecond pulse is focused in a gas, leading to the generation of odd harmonics of the driving field in the extreme ultraviolet (XUV) region and pulse durations in the attosecond regime.[5,6] So far, most HHG pump-probe experiments have been based on a two-color XUV-pump IR-probe approach, with the drawback that the IR pulse might control the dynamics rather than probing them. An alternative approach is to perform XUV-XUV pump-probe experiments, with the added challenge that the XUV pulses then have to be sufficiently intense to allow for the absorption of two or more XUV photons. With photon energies of several tens of eVs the absorption of one photon often leads to single ionization of the target atom, while absorption of a second or more photons can lead to multiple ionization and excitation of the target. Previously, such experiments have been limited to free electron lasers,[7–9] a light source with very high intensity but, so far, reduced time resolution. In the last years intense HHG sources reaching pulse energies in the microjoule range have been developed at FORTH,[10] RIKEN,[11] and recently in our laboratory at the Lund Laser Centre (LLC),[12,13] which are intense enough to perform XUV-XUV pump-probe experiments. So far, only a few HHG-based XUV-XUV pump-probe experiments have been reported,[14–17] and the approach still presents a formidable experimental challenge, requiring simultaneously three critical conditions to be fulfilled: a high XUV intensity, a broad XUV bandwidth and an XUV interferometer with attosecond time resolution.

Here we present the design of a split-and-delay unit for the production of two delayed replicas of an incident XUV pulse. The device features a single grazing incidence reflection in combination with attenuation of remaining IR light co-propagating with the XUV beam, offering a high throughput without the need of introducing additional optics that would further decrease the XUV flux. To achieve the required spatial and temporal stabilities the device is controlled by two PID-controllers monitoring the delay and the beam pointing using an optical reference laser beam. This report is organized as follows: in Section II we present the mechanical design of the split-and-delay unit and discuss how the required specifications are met. In Section III we give details on the feedback and control scheme needed for reliable operation of the device and in Section IV we demonstrate the experimental performance of the unit through a series of tests using a broadband few-cycle IR laser. Finally, we conclude in Section V.

II. MECHANICAL DESIGN

As stated in the Introduction, the split-and-delay unit has to split the XUV pulse in two equal replicas and delay one of them with respect to the other with attosecond resolution, still being able to send them both to the same focusing optics. In addition, in order to guarantee high intensities and short attosecond pulses in the experimental region, the optical components of the device need to feature a high broadband reflectivity in the XUV region.

[a]F. Campi and H. Coudert-Alteirac contributed equally to this work.
[b]E-mail: per.johnsson@fysik.lth.se

To achieve a high broadband reflectivity, we use a single grazing incidence reflection on a silica (SiO_2) substrate, which allows for the transmission of the fundamental IR field. While other designs use collimation of the XUV beam before the split-and-delay unit in order to maintain the spatial overlap in the subsequent focus,[18] our design avoids the use of additional collimating optics which would lower the throughput by the implementation of an active feedback and control scheme, described in Section III. Further, the reflectivity for the IR is minimized by a multi-layer anti-reflection (AR) coating for the IR with *s*-polarization. The coating is designed for a grazing angle of 10° with alternating layers of SiO_2 and TiO_2, the top one being SiO_2, decreasing the IR reflectivity to below 10%. The thickness of the SiO_2 top layer is much larger than the penetration depth of the XUV radiation; therefore, the XUV reflectivity is unchanged by the applied AR coating. At the chosen grazing angle of 10°, the XUV reflectivity of SiO_2 for *s*-polarized light is larger than 50% for photon energies up to 70 eV.

Our mechanical design is based on wavefront splitting, whereas a standard beamsplitter performs the same function through amplitude splitting. In other words, the wave is sent to the edge of two aligned surfaces which are separately reflecting the two halves of the wavefront, creating two replicas of the incoming wave. While other designs usually align the surface edges parallel to the incidence plane (the plane defined by the incoming beam and the surface normal),[16,18] our unit has the surface edges aligned perpendicular to the incidence plane, in order to minimize the fraction of the beam lost between the edges of the plates, ensuring maximum throughput. A similar but less compact design with femtosecond resolution and without the here described PID loop stabilization has recently been implemented for X-rays at the Linac Coherent Light Source free electron laser.[19] The size of the silica plates is 40×14 mm each, so that the combination of the two plates can accommodate a beam diameter of 10 mm at 10° grazing incidence.

The high-intensity HHG beamline is described in detail elsewhere[12,13] but a sketch of the intended inclusion of the split-and-delay unit in the beamline is shown in Fig. 1(a). Briefly, the high-flux XUV pulses together with the generating IR pulses hit the split-and-delay unit at a 10° grazing angle. The IR that is still remaining is blocked completely by a metallic (e.g., aluminum) filter after the split-and-delay unit. The two XUV pulse replicas are finally focused by a short focal length double toroidal mirror in a Wolter configuration, allowing for focusing to a spot size of ~10 μm and intensities in excess of 10^{12} W/cm^2, as recently demonstrated.[13]

A 3D-model of the unit is shown in Fig. 1(b). The unit was designed to meet the requirements of functionality and stiffness, while keeping the maximum flexibility for future upgrades. With this intent the mount is symmetrical with respect to the interface between the two plates in order to be able to use it in different geometry configurations. It is constituted by a base plate (BP) mountable on standard optical posts and two movable parts (MPs), each of them holding one silica plate (SP). The assembly is equipped with three piezoelectric actuators (P-840.3 Physical Instruments, PAs) having a total travel range of 45 μm and three dummy actuators (DAs), which are replicas of the actuator casings without containing piezoelectric actuators. In this way either of the two movable mirror holders could be actuated from the computer, depending on how the split mirror is assembled. Furthermore, there is a possibility of upgrading the design installing six piezoelectric actuators, to have full control of the steering of both the reflected beams. All the real and dummy actuators are directly screwed on the base plate from the back side. The two movable parts are individually held back on the ball tips of the actuators by two extension springs and the contact is made in such a way that the ball tips are resting in the ball tip sockets of manual actuators for standard optics holders (MA). These manual actuators are very finely threaded differential screws, which allow for a pre-alignment of the entire assembly, to a very high precision (25 μm/rev). The actuators are positioned in an "L" shape, so that one of them can control the pivoting point, which can be preset to be right below the reflecting surface of the mirror. This minimizes the coupling between the horizontal and vertical tilt, which can be controlled by means of the other two actuators. The distances between the actuators are such that

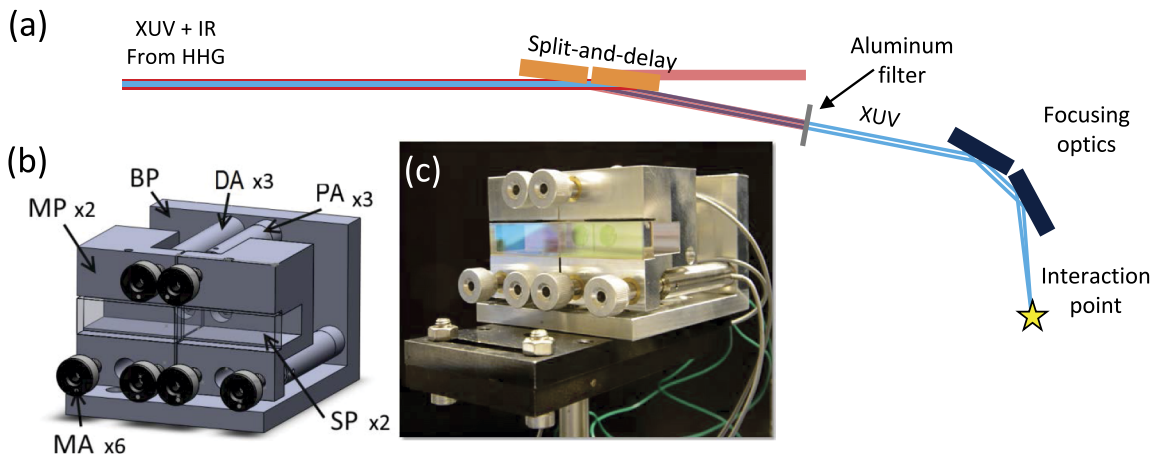

FIG. 1. (a) Sketch of the intended use of the split-and-delay unit in the existing high-intensity XUV beamline. (b) 3D-model of the split-and-delay unit with mounted silica plates. The two movable parts (MPs) are connected to the base plate (BP) by either real piezo-actuators (PA) or dummy actuators (DA), three for each MP. For each connection point there is also a manual actuator (MA) for coarse adjustments. The silica plates (SPs) are held in place by set screws from the top. (c) Photograph of the split-and-delay unit mounted on an optical post for the tests.

the maximum deflection angles are 1.7 mrad and 1.2 mrad in the horizontal and vertical directions, respectively. In our case the achievable delay is not limited by the dimensions of the silica plates since the XUV beam size is much smaller than the 10 mm aperture of the plates. Further, as discussed in Section III, the longitudinal movement of the focus can be neglected, and it is the 45 μm travel range of the piezoelectric actuators that limits the delay range of the device to 52 fs at 10° grazing incidence. Figure 1(c) shows a photo of the assembled device with the silica plates mounted.

III. FEEDBACK AND CONTROL SCHEME

When nonlinear experiments involving the two split replicas, e.g., autocorrelation or pump-probe experiments, have to be performed, not only the temporal delay has to be finely tunable and controlled but also the spatial overlap of the two beams has to be preserved. In the configuration the beamline is designed,[13] after the generation in the gas cell, the harmonic beam propagates over 6 m down to an application chamber. Along this path the beam is diverging before impinging on the split-and-delay unit and keeps diverging down to the application chamber, where the focusing apparatus is installed. Even if the silica plates could be displaced in a perfectly parallel manner not only the delay between the two replicas changes, but the source point of the XUV beam also moves, both laterally and longitudinally. The lateral movement is de-magnified by the focusing optics but, nevertheless, as confirmed by raytracing calculations, a translation of one of the silica plates through its full range (52 fs delay at 10° grazing incidence) leads to an 88 μm movement of the source point which corresponds to a 3 μm movement of the focal spot. This movement, being comparable to the focal spot size, would be detrimental for any pump-probe experiment. In earlier designs this has been remedied by collimating the beam before the split-and-delay unit.[18] In our design, in order to minimize the number of required optics and maintain a high throughput, we have chosen to actively stabilize the overlap of the two replicas in the focus. The longitudinal movement of the source also leads to a longitudinal movement of the focus, but this is so strongly de-magnified by the focusing optics that it becomes negligible. For a translation over the full delay range, as in the example above, the focus moves by less than 20 nm, which is much smaller than the Rayleigh length. Thus, much larger delays could be achieved by replacing the actuators for some with a larger travel.

The optical feedback system uses a green diode laser beam which is made to co-propagate with the main beam using a holey mirror, as illustrated in Fig. 2. After impinging on the split mirror the stabilization beam is constituted by two delayed replicas which are then picked out with another holey mirror and divided in two beams by a beamsplitter. One beam is focused on a camera (overlap control) to monitor the positions of the focal spots of the two replicas, as shown in the top inset of Fig. 2. In the other beam the two replicas are crossed at an angle on another camera (delay control) in order to create an interference pattern like the one shown in the bottom inset of Fig. 2. The phase of the fringes is extracted through Fourier analysis of the recorded image and, since the diode laser wavelength is well-known, from this the relative change in delay between the two replicas can be calculated and used as input to the PID-loop controlling the delay. Before the first holey mirror, a negative lens is used to match the divergence of the diode laser beam with that of the XUV beam, which is crucial for achieving proper control of the spatial overlap of the two replicas in the focus. This is in turn important for ensuring that the crossing angle of the two beams on the delay control camera stays constant. While the current version of the stabilization scheme does not allow for finding the zero delay, this could be achieved through e.g., the interference from a broadband white-light source. For the overlap control, the focal spot positions are recorded and the position of the delayed replica can be tracked by blocking the static replica. This change in the position with respect to the position of the other beam is used as an error function in the PID-loop controlling the two tilts to keep the two replicas overlapped in focus. Figure 3 shows a simplified block diagram of the PID loops implemented in the control software. Pointing and delay controls run asynchronously, each of them updating the piezo-voltages at different rates.

IV. PERFORMANCE TESTS

For the tests of the optical feedback system few-cycle IR pulses with pulse durations down to 5 fs were used instead of

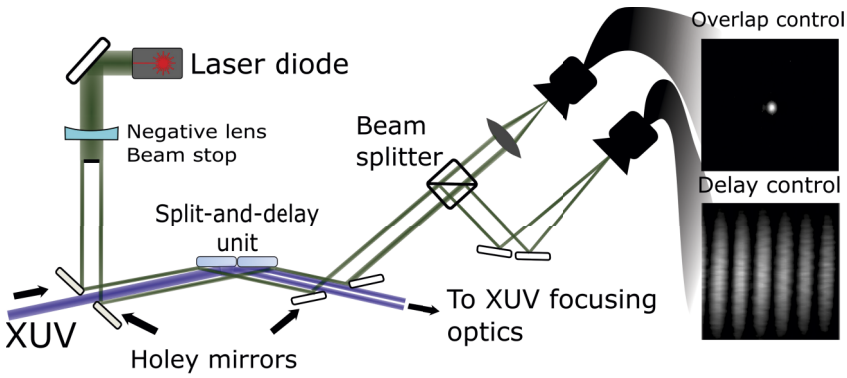

FIG. 2. Setup of the optical feedback system implemented for simultaneously stabilizing delay and overlap in the focus. The insets show images recorded by the overlap control camera (top inset) and the delay control camera (bottom inset).

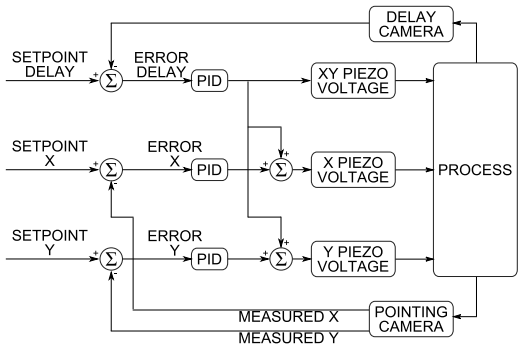

FIG. 3. Block diagram of the pointing and delay control PID loops. The fringes from the "delay camera" are used to measure the delay between the two arms by Fourier analysis, and a PID loop is used to calculate the voltage on the three piezos to get the desired delay. The focus spot from the "pointing camera" is used to monitor the beam position and two PID loops control the voltage applied to the horizontal and the vertical actuators piezos to correct for misalignment. The delay and pointing PID's run asynchronously and can update the piezos voltages at different rates.

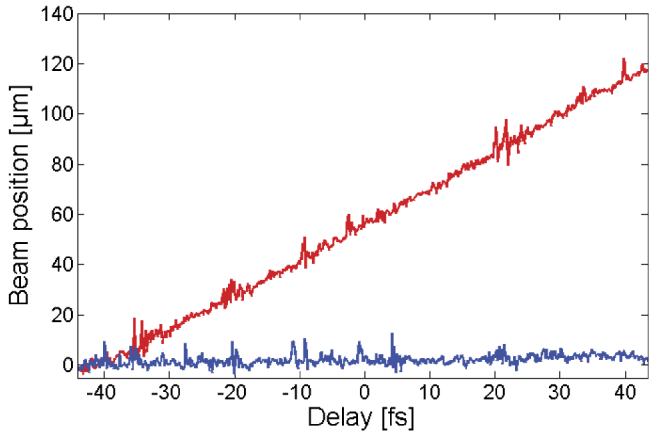

FIG. 4. Horizontal focus position as a function of delay with (blue line) and without (red line) the PID-loop for overlap control.

XUV pulses making it possible to perform the tests outside the vacuum chamber. The IR beam was made to diverge in order to create a virtual source point, and the divergence of the stabilization laser beam was matched to that of the IR. In addition, the unit was used at a larger grazing angle, ≈20°, to obtain a larger delay range. After the split-and-delay unit the IR pulses were focused by a lens with a focal distance of ≈1 m, leading to an IR focal spot of ≈100 μm.

First, the general performance of the feedback and control scheme was tested by placing a beam monitoring camera in the IR focus. The position of the IR focal spot was monitored while scanning over the full delay range. In Fig. 4 the horizontal focus position is shown as a function of delay, with the PID-loop off (red line) and on (blue line). Note that the total delay range in this case is ≈100 fs due to the larger grazing angle used in the test setup than in the XUV setup. Without the PID-loop for overlap control the horizontal position of the focused IR beam moves 120 μm over the full delay range. With the beam geometry used for the test, this corresponds to a movement of the source point of 75 μm, which is consistent with our raytracing simulations. As discussed in Section III, for a future XUV-XUV pump-probe experiment such a source point movement would be detrimental. The stability of the focus position with the PID-loop was 1.9 μm rms which, for the XUV beamline parameters correspond to a stability better than 0.3 μm rms, which is expected to be more than sufficient for future pump-probe experiments. We note that even when the PID loop is running, there are measurements for which the focal spot position deviates with as much as 10 μm from the nominal position. This is still well within the focal spot size of the IR laser, and the corresponding movement of the focal spot for the XUV beamline parameters would be below 2 μm, and thus below the XUV focal spot size.

Second, a pinhole followed by a photodiode was placed in the IR focus and a field autocorrelation scan was recorded. The pinhole was used to increase the contrast by looking only at a tiny portion of the pattern generated by the two replicas. In fact, a standard field autocorrelation is usually performed in a collinear configuration, and when the delay introduces a π phase shift in the relative phase, a minimum is recorded. In our configuration the two replicas have opposite wavefront tilts which produce a time-smearing that, if integrated over the focus, would reduce the contrast of the measurement. Figure 5(a) shows the measured field autocorrelation trace (blue line) and the predicted one (green line) calculated from the measured spectrum of the few-cycle IR pulse, shown in Fig. 5(b).[20] There is a fair agreement between the two, with a slightly lower oscillation frequency for the calculated trace. This is most likely due to the fact that the spectrum of the laser was measured before the setup and will differ slightly from the spectrum with which the trace was recorded, mainly due to the reflectivity of the anti-reflection coating of the silica plates, but possibly also due to the selection of a

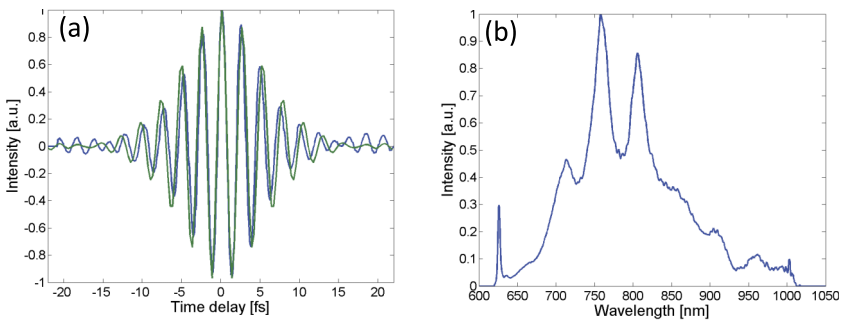

FIG. 5. Field autocorrelation measurement. In panel (a) the measured field autocorrelation trace (blue line) is shown together with the calculated field autocorrelation trace (green line) from the measured spectrum of the few-cycle IR pulse shown in panel (b).

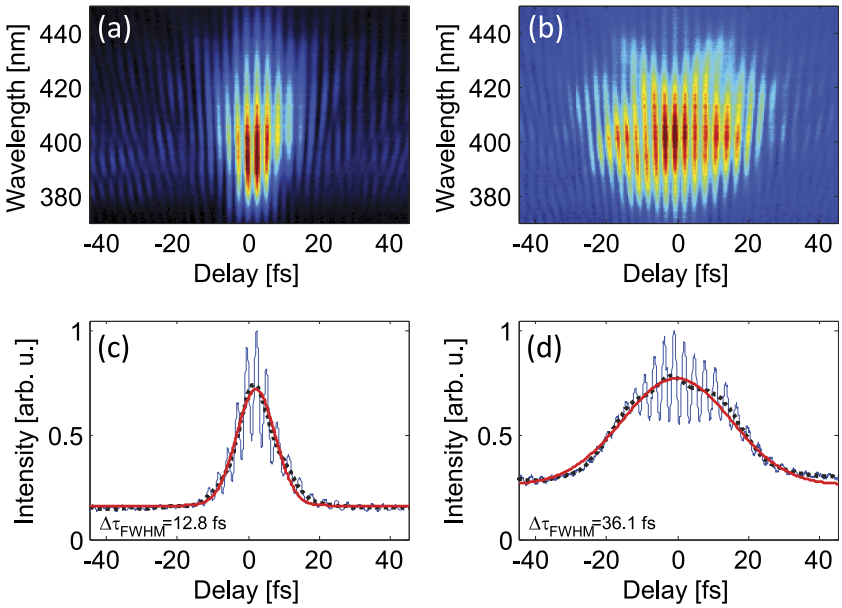

FIG. 6. All-reflective second-order autocorrelation measurement for two different pulse durations, 6.2 fs ((a) and (c)) and 30 fs ((b) and (d)). Panels (a) and (b) show the spectrally resolved measurement and panels (c) and (d) the spectrally integrated signal (blue solid line) and a Gaussian fit (red solid line) to its slowly varying component (black dotted line).

small part of the beam by the pinhole in combination with a small spatial chirp. During the test, the jitter of the PID-loop controlling the delay was estimated to be about 100 mrad rms, corresponding to a delay jitter of 28 as rms. At this point it is worth mentioning that, as discussed above, the actual time resolution obtained in a measurement might be limited by the time-smearing caused by integration over part of the focal plane in combination with the opposite wavefront tilts. If the measurement integrates over the whole focal volume the maximum phase difference will be close to 2π, meaning that the temporal smearing becomes similar to the period of the laser.

After confirming the performance of the feedback scheme, both for the overlap and for the delay, the final test consisted in performing an all-reflective second-order autocorrelation. While a field autocorrelation only contains information about the spectrum of the pulse and no information about the pulse duration, a second-order method allows for extraction of the temporal information. The bandwidth of the pulses used for the tests spans over 300 nm, supporting pulses down to a duration of 5.0 fs. Thus, they are not readily measured by a standard autocorrelation scheme due to intrinsic pulse broadening in the beamsplitter and an all-reflective scheme is necessary. To do this, the pinhole was replaced by a second harmonic generation crystal and a small beam stop was placed in the center of the beam after the crystal for suppressing the intensity autocorrelation component that is preferentially emitted in the forward direction, thus increasing the contrast of the measurement. The signal was then recorded using a fiber-coupled spectrometer for two different pulse durations, and the result is shown in Fig. 6. In Figs. 6(a) and 6(c), the pulses are fully compressed to a duration of 6.2 fs, measured using the d-scan technique,[21] and in Figs. 6(b) and 6(d) the pulse was stretched by material dispersion to a pulse duration of 30 fs. Figs. 6(a) and 6(b) show the spectrally resolved measurement and Figs. 6(c) and 6(d) the spectrally integrated signal.

The traces resemble typical interferometric autocorrelation results but the available scan range is too short compared to the pulse duration to apply a pulse reconstruction algorithm like frequency-resolved optical gating (FROG).[22] We note that the contrast is lower than the 8:1 contrast expected from a collinear second-order interferometric autocorrelation. This is expected since the opposite wavefront tilt of the two replicas, caused by the use of wavefront rather than amplitude division, causes a temporal smearing as the measurement is integrated over the whole focal plane.[23] A low pass frequency filter was applied to the spectrally integrated signal in order to extract the slowly varying signal component. Gaussian fits to this component and deconvolution assuming Gaussian pulse shapes yield pulse durations of 9.1 fs and 25.5 fs for the short and long pulse, respectively, which is in fair agreement with the known pulse durations of 6.2 fs and 30 fs. A possible explanation for the deviation is a narrowing of the bandwidth in the second-harmonic conversion process, which would cause a close to transform-limited pulse to stretch, and a chirped pulse to shorten. In addition, from the Gaussian fits it is clear that, at least the stretched pulse, is not well approximated by a Gaussian.

V. CONCLUSION AND OUTLOOK

In conclusion, we have reported on the design of an all-reflective, grazing incidence, split-and-delay unit for the creation of two time-delayed replicas of an incident XUV pulse. The device has a high broadband throughput, larger than 50% for photon energies up to 70 eV, using a single reflection and combining its function with attenuation of remaining IR light from the HHG process. The device uses two optical feedback loops to maintain spatial overlap and to reach a precise time-resolution. The device was tested using a broadband few-cycle IR laser to perform all-reflective

autocorrelation measurements, demonstrating a delay-jitter below 30 as rms and a spatial overlap stability below 0.3 μm rms. In the near future, the device will be incorporated in our high-intensity HHG beamline with the aim to perform XUV-XUV pump-probe experiments studying attosecond dynamics in atomic and molecular systems.

ACKNOWLEDGMENTS

This research was supported by the Swedish Research Council, the Swedish Foundation for Strategic Research, the Knut and Alice Wallenberg Foundation, the European COST Action CM1204 XLIC, and the European Research Council (PALP). This project has received funding from the European Union's Horizon 2020 research and innovation programme under the Marie Sklodowska-Curie Grant Agreement No. 641789 MEDEA.

[1]L. S. Cederbaum and J. Zobeley, Chem. Phys. Lett. **307**, 205 (1999).
[2]F. Remacle and R. D. Levine, Proc. Natl. Acad. Sci. U. S. A. **103**, 6793 (2006).
[3]F. Calegari, D. Ayuso, A. Trabattoni, L. Belshaw, S. De Camillis, S. Anumula, F. Frassetto, L. Poletto, A. Palacios, P. Decleva, J. B. Greenwood, F. Martin, and M. Nisoli, Science **346**, 336 (2014).
[4]Y. H. Jiang, A. Rudenko, O. Herrwerth, L. Foucar, M. Kurka, K. U. Kühnel, M. Lezius, M. F. Kling, J. van Tilborg, A. Belkacem, K. Ueda, S. Düsterer, R. Treusch, C. D. Schröter, R. Moshammer, and J. Ullrich, Phys. Rev. Lett. **105**, 263002 (2010).
[5]M. Ferray, A. L'Huillier, X. F. Li, L. A. Lompre, G. Mainfray, and C. Manus, J. Phys. B **21**, L31 (1988).
[6]P. Agostini and L. F. DiMauro, Rep. Prog. Phys. **67**, 813 (2004).
[7]N. Berrah, B. Langer, J. Bozek, T. Gorczyca, O. Hemmers, D. W. Lindle, and O. Toader, J. Phys. B **29**, 5351 (1996).
[8]A. Sorokin, M. Wellhöfer, S. Bobashev, K. Tiedtke, and M. Richter, Phys. Rev. A **75**, 051402 (2007).
[9]R. Moshammer, Y. H. Jiang, L. Foucar, A. Rudenko, T. Ergler, C. D. Schröter, S. Lüdemann, K. Zrost, D. Fischer, J. Titze, T. Jahnke, M. Schöffler, T. Weber, R. Dörner, T. J. M. Zouros, A. Dorn, T. Ferger, K. U. Kühnel, S. Düsterer, R. Treusch, P. Radcliffe, E. Plönjes, and J. Ullrich, Phys. Rev. Lett. **98**, 203001 (2007).
[10]N. A. Papadogiannis, L. A. A. Nikolopoulos, D. Charalambidis, G. D. Tsakiris, P. Tzallas, and K. Witte, Phys. Rev. Lett. **90**, 133902 (2003).
[11]E. Takahashi, Y. Nabekawa, and K. Midorikawa, Opt. Lett. **27**, 1920 (2002).
[12]P. Rudawski, C. M. Heyl, F. Brizuela, J. Schwenke, A. Persson, E. Mansten, R. Rakowski, L. Rading, F. Campi, B. Kim, P. Johnsson, and A. L'Huillier, Rev. Sci. Instrum. **84**, 073103 (2013).
[13]B. Manschwetus, L. Rading, F. Campi, S. Maclot, H. Coudert-Alteirac, J. Lahl, H. Wikmark, P. Rudawski, C. M. Heyl, B. Farkas, T. Mohamed, A. L'Huillier, and P. Johnsson, "Two-photon double ionization of neon using an intense attosecond pulse train" (unpublished).
[14]P. Tzallas, D. Charalambidis, N. A. Papadogiannis, K. Witte, and G. D. Tsakiris, Nature **426**, 267 (2003).
[15]Y. Nabekawa, H. Hasegawa, E. J. Takahashi, and K. Midorikawa, Phys. Rev. Lett. **94**, 043001 (2005).
[16]E. J. Takahashi, P. Lan, O. D. Mücke, Y. Nabekawa, and K. Midorikawa, Nat. Commun. **4**, 2691 (2013).
[17]P. Tzallas, E. Skantzakis, L. Nikolopoulos, G. Tsakiris, and D. Charalambidis, Nat. Phys. **7**, 781 (2011).
[18]F. Frassetto, A. Trabattoni, S. Anumula, G. Sansone, F. Calegari, M. Nisoli, and L. Poletto, Rev. Sci. Instrum. **85**, 103115 (2014).
[19]K. R. Ferguson, M. Bucher, J. D. Bozek, S. Carron, J.-C. Castagna, R. Coffee, I. Curiel, M. Holmes, J. Krzywinski, M. Messerschmidt, M. Minitti, A. Mitra, S. Moeller, P. Noonan, T. Osipov, S. Schorb, M. Swiggers, A. Wallace, J. Yina, and C. Bostedt, J. Synchrotron Radiat. **22**, 492 (2015).
[20]Due to the short temporal range of the autocorrelation scan, the acquired trace does not allow for a reconstruction of the spectrum.
[21]M. Miranda, C. L. Arnold, T. Fordell, F. Silva, B. Alonso, R. Weigand, A. L'Huillier, and H. Crespo, Opt. Express **20**, 18732 (2012).
[22]R. Trebino, K. W. DeLong, D. N. Fittinghoff, J. Sweetser, M. A. Krumbügel, and B. Richman, Rev. Sci. Instrum. **68**, 1 (1997).
[23]P. Tzallas, D. Charalambidis, N. A. Papadogiannis, K. Witte, and G. D. Tsakiris, J. Mod. Opt. **52**, 321 (2005).